View Article Online
DOI: 10.1039/C8TA03280G

Evaporation above a bulk water surface using an oil lamp inspired highly efficient solar-steam generation strategy

Xuan Wu,[a†] Limin Wu,[a†] Jeanette Tan,[a,b] George Y. Chen,[c] Gary Owens,[a] Haolan Xu*[a]

[a] Future Industries Institute, University of South Australia, Mawson Lakes Campus, SA 5095, Australian.

[b] School of Natural and Built Environments, University of South Australia, Mawson Lakes Campus, SA 5095.

[c] School of Engineering, University of South Australia, Mawson Lakes Campus, SA 5095, Australia

[†] These authors contribute equally to this work

* E-mail: haolan.xu@unisa.edu.au

Published on 06 June 2018. Downloaded by UNIVERSITY OF SOUTH AUSTRALIA on 08/06/2018 02:58:14.

Journal of Materials Chemistry A Accepted Manuscript

View Article Online
DOI: 10.1039/C8TA03280G

Published on 06 June 2018. Downloaded by UNIVERSITY OF SOUTH AUSTRALIA on 08/06/2018 02:58:14.

Abstract

Inspired by the traditional oil lamp, a solar-steam generation system with an evaporation surface located above the bulk water surface is realized using a cotton strand coated with a photothermal layer of polydopamine as a wick. The strong wicking effect of the cotton strand is able to transfer significant amount of water rapidly to the evaporation surface > 9 cm above the bulk water surface. The capability to separate the evaporation surface from the bulk water is highly advantageous as it decreases the dissipation of heat into the bulk water. This leads to a highly localized light-to-heat energy conversion, which results in an outstanding solar-steam generation performance. The energy conversion efficiency for the water evaporation system reaches 88.8% under 1.0 sun irradiation. The system was applied to decrease the salinity of seawater, demonstrating that clean water could be produced from salty water via evaporation with residual Na concentration of only ~0.31 ppm under 1.0 sun. The proposed strategy is simple and the optimized design does not require photothermal materials to float on water surface, but is rather allowed photothermal material to be fixed a considerable distance above the water surface. The overall system is both natural and cost effective and thus shows great potential for real-world applications particularly in developing countries where natural resources are already stretched and access to clean drinking water is not guaranteed.

Keywords: cotton, oil lamp, photothermal, polydopamine, water evaporation

Journal of Materials Chemistry A Accepted Manuscript

View Article Online
DOI: 10.1039/C8TA03280G

Published on 06 June 2018. Downloaded by UNIVERSITY OF SOUTH AUSTRALIA on 08/06/2018 02:58:14.

Journal of Materials Chemistry A Accepted Manuscript

Introduction

Before the invention of electricity and the incandescent light bulb, kerosene oil lamps were commonly used for illumination. A basic oil lamp consists of three simple components a wick, a fuel chamber, and a fuel. The wick delivers the fuel by capillary action, from fuel chamber to its tip where the fuel is burned and light is generated. Thus the fire and the bulk of the fuel are linked but spatially separated by the wick, which guarantees a continuous supply of fuel at a modest rate allowing for sustained combustion while simultaneously safely maintaining separation of the flame and the fuel chamber. The distance between the fire and bulk fuel effectively hinders heat transfer from the burning surface to the fuel thus avoiding explosive ignition. This working mechanism is reminiscent of those used in the recently developed solar-steam generation systems.[1-18] Typically, photothermal materials (PTMs) are placed on a water surface (i.e. at the air-water interface) to absorb solar light and convert it into heat, thereby heating up and evaporating absorbed water. One of the most important strategies to improve the energy utilization efficiency is to localize heat on the surface of the PTMs. This is generally realized by using PTMs of low thermal conductivity which effectively hinder heat transfer from the PTM surface to the bulk water. While PTMs could simply be dispersed into the bulk water, floating them on the water surface has been shown to dramatically suppress heat dissipation, leading to superior solar-steam generation performance.[19-32] However, some heat loss due to the direct contact between the PTM and bulk water is inevitable. To minimize this heat loss, increased spatial separation of the PTM surface (i.e. the evaporation surface) and the bulk water is required, while maintaining efficient transportation of water from the bulk water to the evaporation surface.[33,34] Recently, Zhu and co-workers successfully developed a 3D artificial transpiration device to separate the evaporation surface and bulk water. The device was composed of a 3D hollow cone light absorber and a 1D water path. Due to the indirect contact between the photothermal hollow cone and bulk water, a high solar steam generation efficiency of 85% was achieved.[33] Another solar-thermal evaporation

View Article Online
DOI: 10.1039/C8TA03280G

Published on 06 June 2018. Downloaded by UNIVERSITY OF SOUTH AUSTRALIA on 08/06/2018 02:58:14.

system was designed by placing photothermal materials on top of a polystyrene foam wrapped by a layer of cellulose. The foam physically separated the photothermal layer and the bulk water, while the cellulose layer enabled a 2D water path for water supply.[34] These two designs significantly supressed the heat loss and led to excellent performance in water evaporation. The devices are composed of at least two functional parts, a photothermal water evaporation surface and a water path/physical separator. It is expected that using a single part with the both functions would simplify the system. Herein, inspired by the traditional wick-based oil lamp, a lamp-like solar evaporation system was developed with negligible heat dissipation from the evaporation surface to the bulk water. Cotton strands coated with photothermal layers were used as the "wick" and highly efficient solar evaporation above the bulk water surface was successfully demonstrated.

Cotton is a common and cheap material, which is widely used for the manufacture of a variety of fabrics. Cotton has an extremely low thermal conductivity of only ~0.04 W m^{-1} K^{-1}. The commercial degreasing cotton is hydrophilic. Thus, cotton fabric is wearable, washable at high temperatures and capable of adsorbing moisture. More importantly, cotton as a common raw material for clothing is environmentally friendly and non-toxic. All of these characteristics make cotton an ideal material for water treatment via solar-thermal water evaporation. However, cotton itself is not a good photothermal material and cannot effectively absorb sunlight and produce heat to thereafter evaporate water. Herein, carbonization and photothermal coating with polydopamine (PDA) were used to render the cotton photothermally active. PDA, is the main constituent of proteins in the adhesive plaque of mussels, which can be grown on any substrate simply by self-polymerization of dopamine (monomer) in alkaline solution.[35-40] Concomitantly, PDA is an excellent photothermal material with an adsorption range spanning across UV, visible and even near-infrared regions.[11, 41] These two beneficial characteristics suggest that PDA can be easily coated on

Journal of Materials Chemistry A Accepted Manuscript

View Article Online
DOI: 10.1039/C8TA03280G

Published on 06 June 2018. Downloaded by UNIVERSITY OF SOUTH AUSTRALIA on 08/06/2018 02:58:14.

cotton and thereby impart excellent photothermal performance to the cotton thus realizing the "wick" in the kerosene lamp-like solar-thermal water evaporation system. Since cotton and PDA are both natural, cost effective and biodegradable materials, they are well suited for applications in solar-thermal water treatment.

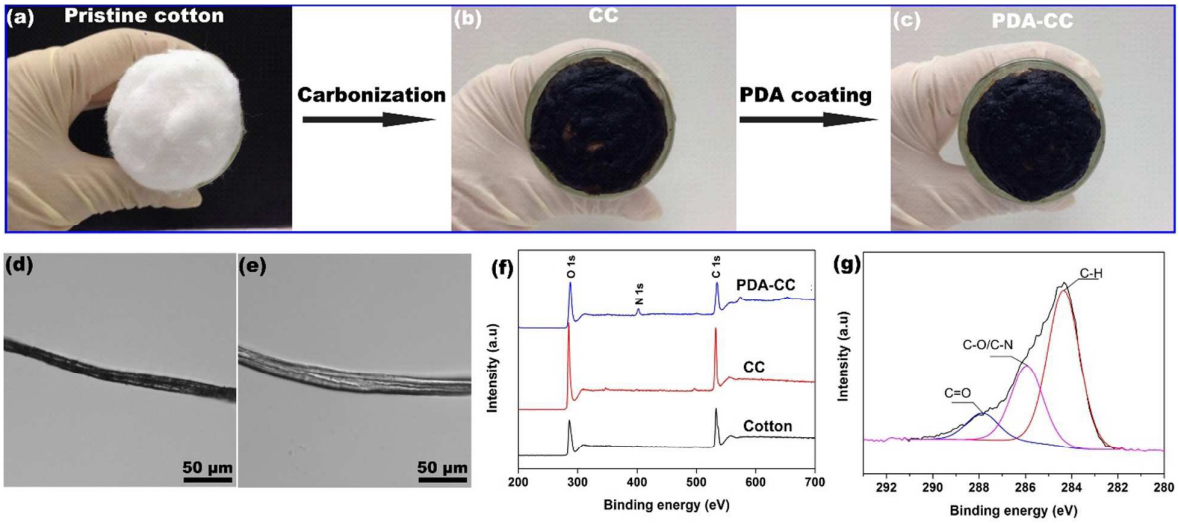


Fig. 1 Digital photographs of pristine cotton (a), carbonized cotton (b) and PDA-CC (c) together with optical microscopy images of a PDA coated cotton fiber before (d) and after (e) water adsorption. XPS survey spectra of the pristine cotton, CC and PDA-CC (f), and high-resolution XPS spectrum of C 1s for PDA-CC (g).

Results and discussion

Since pristine white cotton cannot effectively absorb light, it must first be modified for application in solar steam generation. Initially pristine cotton underwent carbonization by a flame which changed the colour from white (Fig. 1a) to black (Fig. 1b), indicating formation of carbonaceous substances and the enhancement of light absorption. Subsequently, a PDA layer was formed on the surface of the carbonized cotton (CC) by a facile self- polymerization of dopamine.[11, 31] The PDA coated CC (PDA-CC) further enhanced the light absorption as evidenced by the perceivable darker colour (Fig. 1c). The pristine commercial degreasing cotton is hydrophilic as a water droplet can be absorbed into the cotton immediately upon

Journal of Materials Chemistry A Accepted Manuscript

View Article Online
DOI: 10.1039/C8TA03280G

Published on 06 June 2018. Downloaded by UNIVERSITY OF SOUTH AUSTRALIA on 08/06/2018 02:58:14.

contact (Supporting information Video S1). Carbonization of pristine cotton makes the surface relatively hydrophobic so that when a water droplet was placed on the surface of CC, it took ~5 s to penetrate the surface (Supporting information Video S2). However, coating the CC surface with a PDA layer reinstated hydrophilicity. When a water droplet was placed on the surface, it was absorbed into the PDA-CC much more quickly, within 0.2 s (Supporting information Video S3), This result confirmed the superhydrophilicty of the PDA coating which has the benefit of forming very thin water films on the PTM surface allowing for fast solar-thermal evaporation.[11] Optical microscopy images of a PDA coated cotton fiber before (Fig. 1d) and after (Fig. 1e) water absorption were recorded to roughly estimate the thickness of water film formed on the fiber surface (see the experimental set in Figure S1). It is noticed that the diameter of the fiber increased by about 6.2 μm after water wetting. Considering that the cotton fiber may swell after water absorption, it is reasonable to infer that the thickness of the water film formed on the fiber surface was less than 3.1 μm. It is expected that such a thin film of water can be heated and rapidly evaporated by the photothermal PDA-CC under light irradiation.

X-ray photoelectron spectroscopy (XPS) analysis of the cotton, CC and PDA-CC was conducted to elucidate the elements present on the surface and their chemical states. The XPS survey spectra (Fig. 1f) shows that the major elements present in cotton and CC were carbon (C) and oxygen (O). For pristine cotton, the carbon content was 73.1% and the oxygen content was 26.2%, corresponding to a C/O ratio of 2.79. After carbonization, carbon content increased slightly to 77.1% and the oxygen content decreased to 20.6 % corresponding to an increase in the C/O ratio to 3.74. The N content of both pristine cotton and CC are very low (0.28% for cotton and 0.84% for CC), which originated from residual proteinous compounds in cotton cellulose. In sharp contrast the N content of PDA-CC was 5.7%, which confirmed that PDA had been successfully coated onto the surface of CC. The C 1s peak of the PDA-CC

Journal of Materials Chemistry A Accepted Manuscript

View Article Online
DOI: 10.1039/C8TA03280G

Published on 06 June 2018. Downloaded by UNIVERSITY OF SOUTH AUSTRALIA on 08/06/2018 02:58:14.

can be deconvoluted to give peaks attributed to C=O (287.5 eV), C-N/C-O (285.5 eV) and C-H (284.3 eV) (Fig. 1g), which correspond to the major peaks expected for PDA.[31]

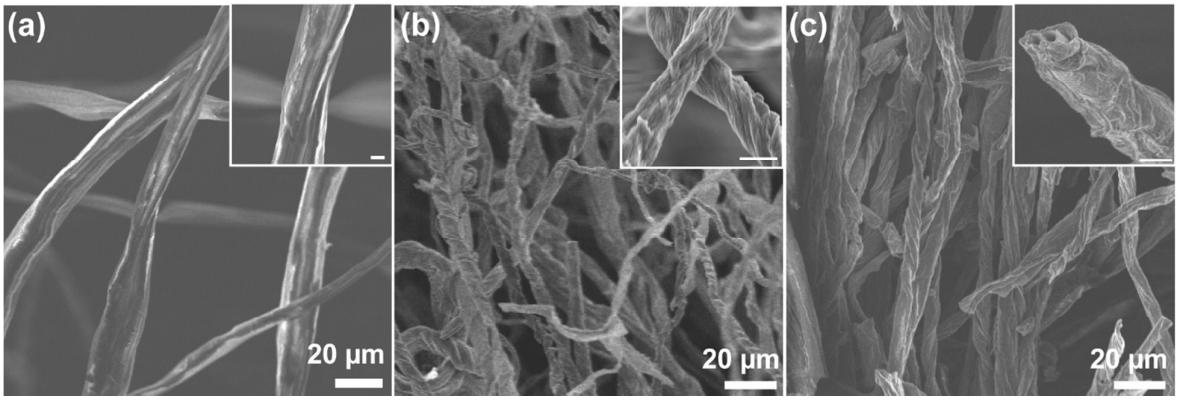


Fig. 2 SEM images of pristine cotton (a), CC (b) and PDA-CC (c). Upper insets are the magnified SEM images showing more detailed surface feature of the fibers, where the scale bar in the inset corresponds to 3 μm.

Scanning electron microscopy (SEM) images recorded the morphological and surface structure change of the cotton before and after treatment. Pristine cotton was composed of fibers with a slightly twisted ribbon-like morphology (Fig. 2a) with a mean fiber diameter of ~18.2 ± 2.4 μm. The surface was relatively smooth (upper inset, Fig. 2a). After carbonization, the average diameter of the fibers dramatically decreased to 4.9 ± 0.9 μm (Fig. 2b). The shrinkage was due to the removal of flammable compounds during burning of the fibers. The carbonized fibers were more heavily twisted than that of pristine cotton, and the surface of fibers became very rough (Upper inset, Fig. 2b). It is believed that roughness can enhance light absorption for light-to-heat conversion,[42, 43] and simultaneously increase the surface area for water evaporation. Finally coating of PDA on the surface of CC led to a slight increase in the average diameter to 5.8±1.0 μm (Fig. 2c), while preserving the twisted helical structure. The observed surface of PDA-CC was significantly different from CC, with a wrinkle polymer-like surface structure, which is characteristic of the formation of a thick PDA layer.

Journal of Materials Chemistry A Accepted Manuscript

View Article Online
DOI: 10.1039/C8TA03280G

Published on 06 June 2018. Downloaded by UNIVERSITY OF SOUTH AUSTRALIA on 08/06/2018 02:58:14.

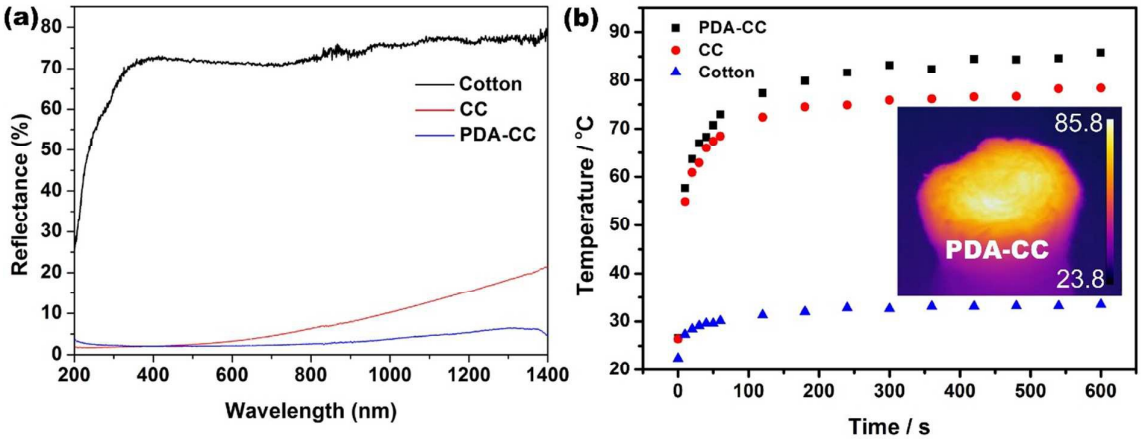


Fig. 3 (a) Diffusive reflectance spectra of pristine cotton (black curve), CC (red curve) and PDA-CC (blue curve). (b) Time-dependent surface temperature curve of pristine cotton, CC and PDA-CC under 1.0 sun irradiation, inset: IR image of the PDA-CC.

The ability of a PTM to absorb light is a key factor in determining that material's performance. Carbonization and PDA coating of a cotton significantly enhanced light absorption capability. While pristine cotton has a strong reflectance (71-76%) in the wavelength range of 350-1400 nm (Fig. 3a), corresponding to appeared strong white colour and weak photothermal effect. Carbonization successfully suppressed reflectance from the cotton surface. Thus the UV-vis spectrum showed that the reflectance of CC dramatically decreased to < 2.0% and < 6.3% in the UV (200-400 nm) and visible (400-780 nm) regions respectively and the maximum reflectance was still only about 20% at 1400 nm. Application of a PDA coating on CC further lowered the reflectance to <2.5% over the visible ranges (300-780 nm), and to < 6.2% at higher wavelengths (800-1400 nm). Therefore, since PDA-CC is completely opaque (no transmittance loss), PDA-CC can absorb almost all of the incident sunlight in the UV-visible (>97.5%) and NIR (>93.8%) spectral regions. It is comparable with most of the reported excellent photothermal materials for water evaporation and semiconductor materials for photodetector.[44,45] The presence of carbonaceous substances, PDA, as well as surface roughness all contribute to a high light absorption efficiency. While high light absorption

Journal of Materials Chemistry A Accepted Manuscript

View Article Online
DOI: 10.1039/C8TA03280G

Published on 06 June 2018. Downloaded by UNIVERSITY OF SOUTH AUSTRALIA on 08/06/2018 02:58:14.

ability is the most important factor governing light-to-heat conversion, the thermal conductivity of the PTM determines the final surface temperature. Materials with a lower thermal conductivity have the benefit of concentrating and localizing of the generated heat on the surface of the PTM. Since cotton has a very low thermal conductivity (0.04 W m^{-1} K^{-1}) when modified to produce PDA-CC, this can be combined with excellent light absorption abilities to deliver a high surface temperature under light irradiation. To verify this, pristine cotton, CC and PDA-CC were placed under a solar simulator with a light intensity of 1.0 kW m^{-2} (equal to 1.0 sun). Then, the variation in surface temperature was monitored as a function of irradiation time using an IR camera. The emissivity (ε) of the cotton for thermal imaging estimation of surface temperature is 0.77, while the emissivity of CC and PDA-CC surfaces were measured to be about 0.85 and 0.80 (see details in experimental section in Supporting Information). Under 1.0 sun irradiation, the surface temperature of cotton slowly increased and reached an equilibrium of ~33.2 ^{o}C after 3 min of irradiation (Fig. 3b, S2a). In comparison, the surface temperature of CC and PDA reached a maximum of about 78.4 ^{o}C and 85.8 ^{o}C after 5 min of irradiation (Fig. 3b, S2b).

To realize our concept of lamp-like water evaporation (Fig. 4a), we utilized a plastic cylinder to hold water while a cap with a hole was used to secure the cotton strands (Fig. 4b, Fig. S3). The initial distance *D* between the evaporation surface (i.e. the top surface of cotton strand) and the bulk water level was set as 6 cm. Owing to the excellent wicking effect, the cotton strand continuously delivered water from bulk phase to the top of the PTM surface, just like in an oil lamp. This non-direct-contact solar evaporation effectively negates significant heat dissipation from the evaporative PTM surface to the bulk water, allowing localization of heat for more

Journal of Materials Chemistry A Accepted Manuscript

View Article Online
DOI: 10.1039/C8TA03280G

Published on 06 June 2018. Downloaded by UNIVERSITY OF SOUTH AUSTRALIA on 08/06/2018 02:58:14.

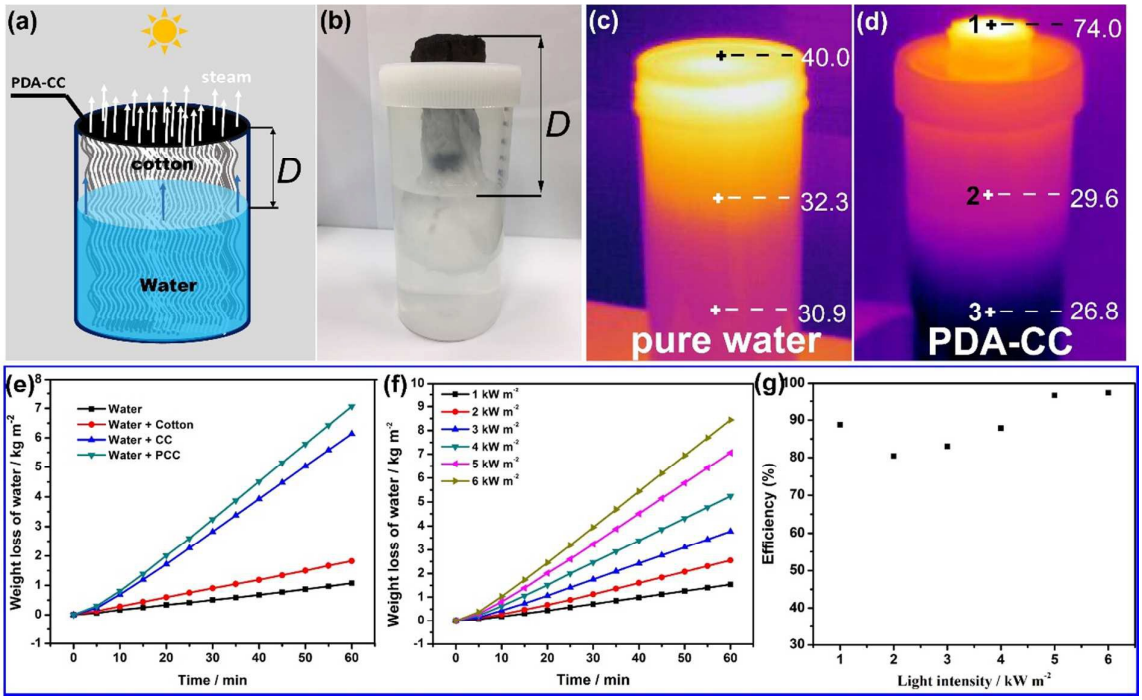


Fig. 4 Schematic illustration of the lamp-like solar water evaporation system (a) and a coressponding digital photo of the actual lamp-like solar steam generation system (b). IR image of the solar steam system 30 min after 5.0 sun irradation with pure water (c) PDA-CC and water (d). Time-dependent mass loss of water in presence of cotton, CC and PDA-CC under 5.0 sun irradiation (e). Time-dependent weight loss of water in presence of PDA-CC under 1.0, 2.0, 3.0, 4.0, 5.0 and 6.0 sun irradiation (f) and the corresponding evaporation efficiency η (g).

efficient water evaporation. This effect was convincingly demonstrated by the measured temperature gradient of the evaporation system under strong solar simulator irradiation (5.0 sun). With the PDA-CC serving as the wick, after irradiation for 30 min, the surface temperature of PDA-CC had already reached 74.0 ^{o}C (Fig. 4d and Fig. S4), while the temperature of the cotton under the evaporation surface (spot 2) and bulk water (spot 3) was only 29.6 ^{o}C and 26.8 ^{o}C respectively (Fig. 4d). However, without PDA-CC, the variation in temperatures with height was not significant (Fig. 4c), and the bulk water was heated up to

Journal of Materials Chemistry A Accepted Manuscript

View Article Online
DOI: 10.1039/C8TA03280G

Published on 06 June 2018. Downloaded by UNIVERSITY OF SOUTH AUSTRALIA on 08/06/2018 02:58:14.

30.9 ^{o}C. This confirmed that the lamp-like solar-steam system is capable of concentrating the heat converted from light at the PTM surface for efficient water evaporation.

The evaporation rate over pure water, cotton, CC and PDA-CC were tested. Under 5.0 sun irradiation, a substantial amount of steam was generated (Fig. S5). The evaporation rate was calculated based on the time-dependent weight loss curves. Under 5.0 sun irradiation, the evaporation rate was 1.08 kg m^{-2} h^{-1} for a water blank, 1.83 kg m^{-2} h^{-1} for cotton, 6.14 kg m^{-2} h^{-1} for CC and 7.06 kg m^{-2} h^{-1} for PDA-CC. Thus the water evaporation over PDA-CC was much faster, up to 5.5 times higher than evaporation observed in the water blank. For PDA-CC, the evaporation rate under different light intensity was investigated resulting in the calculated evaporation rates of 1.54, 2.55, 3.78, 5.23, 7.06, and 8.44 kg m^{-2} h^{-1} under light intensities of 1.0, 2.0, 3.0, 4.0, 5.0 and 6.0 suns respectively.

To assess the percentage of the solar flux that been utilized to evaporate water, the solar-steam generation efficiency (η) was then calculated using the following equation:

$$\eta = \frac{m(H_{Lv}+Q)}{E_{in}} \qquad (1)$$

Where m is the water evaporation rate ($kg \cdot m^{-2} \cdot h^{-1}$) (with dark evaporation over the samples subtracted, 0.26 kg m^{-2} h^{-1} for PDA-CC), H_{LV} is the total enthalpy that is required to cause the transition of water from its liquid to vapor phase ($H_{Lv}(T)$=1.91846 × $10^6[T/(T\text{-}33.91)]^2$ J/kg), T is the temperature of evaporation, Q is the sensible heat of water of unit mass ($Q = c(T\text{-}T_1)$ J/Kg), where c is the specific heat of water which is 4.2 J/gK, T_1 is the initial temperature of water, and E_{in} ($kJ \cdot m^{-2} \cdot h^{-1}$) is the energy input of the incident light. The results show that the η over PDA-CC reaches 88.8% at 1.0 sun irradiation and 80.5%, 83.0%, 87.9%, 96.5% and 97.2% at 2.0, 3.0, 4.0, 5.0 and 6.0 sun irradiation respectively. Considering the high η, simple evaporation system set-up and low material cost, this lamp-like solar-evaporation system has great potential for practical applications.

Journal of Materials Chemistry A Accepted Manuscript

View Article Online
DOI: 10.1039/C8TA03280G

Published on 06 June 2018. Downloaded by UNIVERSITY OF SOUTH AUSTRALIA on 08/06/2018 02:58:14.

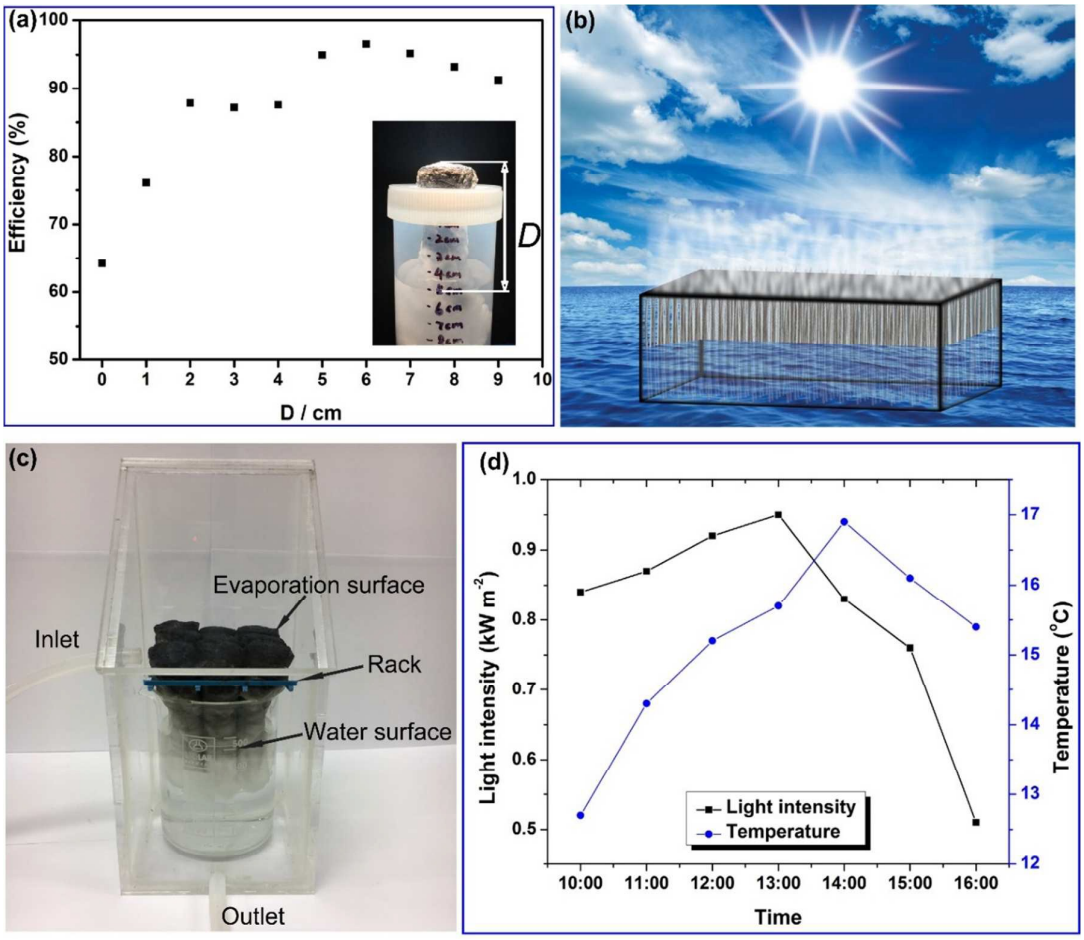


Fig. 5 (a) Solar evaporation efficiency η as a function of D between the evaporation surface and bulk water surface, inset: digital photograph of a test set. (b) Illustration of the expected solar-evaporation system with evaporation surface located above the water surface for real-world application. (c) Photography of a designed solar-thermal water evaporation device. (d) Light intensity and ambient temperature along with time for outdoor test.

One of the unique advantages of this lamp-like evaporation system is that the evaporation surface is able to be located well above the bulk water surface (Fig. **5**a inset). Therefore, the generated heat can be concentrated on the PDA-CC surface to heat the thin water film (<3.1 μm in thickness), leading to a rapid water evaporation. Steam was observed only ~10 s after light irradiation was applied (Supporting information, Video S4). Another advantage of this system is that it is not necessary to float the PTMs on the water surface, thus widening the

Journal of Materials Chemistry A Accepted Manuscript

View Article Online
DOI: 10.1039/C8TA03280G

Published on 06 June 2018. Downloaded by UNIVERSITY OF SOUTH AUSTRALIA on 08/06/2018 02:58:14.

applicable materials that can be used and the PDA-CC strand could be fixed above the surface with a simple mechanical support (Fig. 5b). However, it is not known at what distance (*D*), between the evaporation surface and bulk water surface, is optimal for enhanced evaporation. To investigate this issue, solar-evaporation was investigated at different *D* (0, 1, 2, 3, 4, 5, 6, 7, 8, 9 cm) under 5.0 sun irradiation, where 0 cm means that the evaporation surface was at the same level as the bulk water surface. As show in Fig. 5a and Fig. S6, initially, the water evaporation at *D*=0 was the lowest at 4.67 $kg \cdot m^{-2} \cdot h^{-1}$, corresponding *to* η = 64.2%. This is because the heat converted from the light can be easily dissipated to the bulk water, as the PTM evaporation surface is in direct contact with the bulk water at this height. It was reasonable to assume that as *D* increased, less heat loss by diffusion to the bulk water would occur and more heat would be available for water evaporation, leading to a higher water evaporation rate and η. As expected as *D* increased from 0 to 6 cm, the η increased from 64.2% to 96.5%. However, further increase of *D* > 6 cm caused decrease in η. For example, at *D* = 7, 8, and 9 cm, η decreased to 95.2%, 93.2% and 91.3% separately. This may be because at larger *D*, the water transportation rate from the bulk water along the cotton strand to the evaporation surface is lower than the solar-evaporation rate, thus limiting the overall rate of water evaporation. The wicking rate can be estimated by the Lucas-Washburn equation:

$$D = k\sqrt{t} \tag{2}$$

$$k = \sqrt{\frac{\gamma d \cos\theta}{4\mu}} \tag{3}$$

Where *D* is the distance the liquid travelled, *t* is the time, *k* is the constant characteristic of the cotton-liquid system, γ is surface tension, *d* is diameter of the space between the cotton fibers, θ is contact angle between water and cotton surface, and μ is the viscosity of water. In our case, because the inflection point of evaporation rate is at *D* between 6-7 cm, it is reasonable to assume that at this height, the *t* for transporting a certain amount of water by wicking, is

Journal of Materials Chemistry A Accepted Manuscript

View Article Online
DOI: 10.1039/C8TA03280G

Published on 06 June 2018. Downloaded by UNIVERSITY OF SOUTH AUSTRALIA on 08/06/2018 02:58:14.

similar to the *t* for evaporating the same amount of water. When *D* was increased, according to equation (2), the *t* for water transportation by wicking also increased. Meaning that for the same time period *t* as *D* increased, the amount of wicked water to the PTM surface was reduced. As a direct consequence, the evaporated water reduced, led to a decreased solar evaporation rate.

To evaluate the performance of the lamp-like solar evaporation system for practical application, we designed and fabricated a solar desalination device. As shown in Fig. 5c, the device is composed of a water container and a condensation chamber. PDA-CC strands were supported by a rack on top of the water container. The evaporation surface (i.e. PDA-CC surface) was located above the bulk water surface. Outdoor test was conducted, the weather conditions including light intensity and ambient temperature were recorded and showed in Fig. 5d. Note the light intensity and temperature was quite low due to the winter season in Adelaide, Australia. The test was performed from 10 am to 4 pm. The average clean water production is about 1.12 $kg \cdot m^{-2} \cdot h^{-1}$.

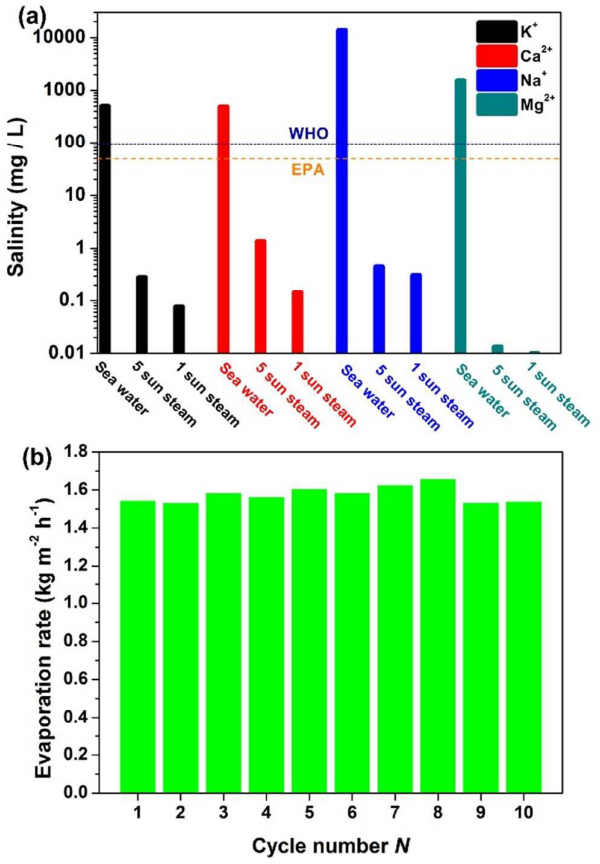
Finally, the feasibility of applying the lamp-like solar-steam generation system for desalination was tested via assessment of the evaporation of real seawater.[23,29,30,34,46,47] The concentration of Na^+, K^+, Ca^{2+} and Mg^{2+} in the generated steam was collected and analyzed by an inductively-coupled plasma-mass spectrometry. As shown in Fig 6a the concentration of Na^+ in the collected water was only 0.31 ppm and 0.45 ppm when the light intensity was 1.0 and 5.0 suns, respectively. The salinities of all the samples are much lower than the salinity level of the drinkable desalination water defined by World Health Organization (WHO) and US Environmental Protection Agency (EPA) Standard, confirming that this evaporation system is applicable for solar-thermal desalination.[23] For the real-world desalination, design of salt resistant photothermal materials is vitally imporant.[29] During evaporation, salt ions are transported by advection to the photothermal material surface and

Journal of Materials Chemistry A Accepted Manuscript

View Article Online
DOI: 10.1039/C8TA03280G

Published on 06 June 2018. Downloaded by UNIVERSITY OF SOUTH AUSTRALIA on 08/06/2018 02:58:14.

are continuously concentrated there within the water film, resulting in the build-up of a high salt concentration on evaporation surface and a salt concentration gradient from the top to bottom within the channels/pores of the photothermal materials. The concentrated salt ions diffuse towards the bottom of the photothermal materials (i.e. bulk water), offsetting the salinity increase on the top surface. The dynamic competition between these two effects determines whether salt crystallization occurs. In our case, there is no salt deposition on PDA-CC surface, indicating that the salt ion transportation by diffusion is faster that that by advection. We suppose that the open water paths formed between the cotton fibers provide massive ion diffusion pathways and a high diffusion capacity, thus hindering the saturation of salt ions on the PDA-CC surface. The stability of the PDA-CC for solar-steam generation was also assessed under 1.0 sun irrdation. As shown in Fig 6b, the evaporaiton rates are similar during the 10 cycles.



Journal of Materials Chemistry A Accepted Manuscript

View Article Online
DOI: 10.1039/C8TA03280G

Fig. 6 (a) Ion concentration of the original seawater and the clean water after solar-thermal desalination. (b) Evaporation rates over PDA-CC of 10 cycles under 1.0 sun irradiation.

In summary, inspired by the kerosene oil lamp, an advanced solar-evaporation system with high evaporation efficiency was demonstrated. A carbonized cotton strand coated with PDA was used as a wick to enable solar evaporation above the bulk water surface. Due to the excellent photothermal effect of PDA, the low thermal conductivity of cotton, the spatial separation between the evaporation surface and the bulk water, as well as the very thin water film on the evaporation surface, highly efficient solar-thermal evaporation was realized. The steam can be generated quickly after only about 10 s of light irradiation (5.0 sun). The solar-evaporation efficiency reached 88.8% under 1.0 sun irradiation. For the bench scale system developed here, the best evaporation efficiency occurred when *D* was 6 cm. The system was applicable for the desalination of seawater since the salinity of the produced clean water was only ~0.31 ppm under 1.0 sun irradiation. All the materials used are natural, cost effective and biodegradable which paves the way for a variety of real-world applications in the future.

Supporting Information
Supporting Information is available online or from the author.

Conflict of interest: The authors declare no competing financial interest

Acknowledgment. The authors thank for the finical support from the Future Industries Institute, University of South Australia (Foundation Fellow), and Huasheng Graphite Co., Ltd.

References:

1. L. M. Tian, J. Y. Luan, K. K. Liu, Q. S. Jiang, S. Tadepalli, M. K. Gupta, R. R. Naik and S. Singamaneni, *Nano Lett.*, 2016, **16**, 609-616.
2. Y. Liu, J. W. Lou, M. T. Ni, C. Y. Song, J. B. Wu, N. P. Dasgupta, P. Tao, W. Shang and T. Deng, *ACS Appl. Mater. Interfaces*, 2016, **8**, 772-779.
3. N. S. Lewis, *Science*, 2016, **351**, 353.
4. S. Ishii, R. P. Sugavaneshwar and T. Nagao, *J. Phys. Chem. C*, 2016, **120**, 2343-2348.

Published on 06 June 2018. Downloaded by UNIVERSITY OF SOUTH AUSTRALIA on 08/06/2018 02:58:14.

Journal of Materials Chemistry A Accepted Manuscript

View Article Online
DOI: 10.1039/C8TA03280G

Published on 06 June 2018. Downloaded by UNIVERSITY OF SOUTH AUSTRALIA on 08/06/2018 02:58:14.

5. D. W. Zhao, H. Z. Duan, S. T. Yu, Y. Zhang, J. Q. He, X. J. Quan, P. Tao, W. Shang, J. B. Wu, C. Y. Song and T. Deng, *Sci. Rep.*, 2015, **5**, 17276.
6. L. B. Zhang, B. Tang, J. B. Wu, R. Y. Li and P. Wang, *Adv. Mater.*, 2015, **27**, 4889-4894.
7. Q. S. Jiang, H. G. Derami, D. Ghim, S. S. Cao, Y. S. Jun, S. Singamanei, *J. Mater. Chem. A*, 2017, **5**, 18397-18402.
8. O. Neumann, A. D. Neumann, E. Silva, C. Ayala-Orozco, S. Tian, P. Nordlander and N. J. Halas, *Nano Lett.*, 2015, **15**, 7880-7885.
9. Y. Ito, Y. Tanabe, J. H. Han, T. Fujita, K. Tanigaki and M. W. Chen, *Adv. Mater.*, 2015, **27**, 4302-4307.
10. K. Bae, G. Kang, S. K. Cho, W. Park, K. Kim and W. J. Padilla, *Nat. Commun.*, 2015, **6, 10103**.
11. X. Wu, G. Y. Chen, W. Zhang, X. Liu and H. Xu, *Adv. Sustainable Syst.*, 2017, **1**, 1700046.
12. M. W. Zhu, Y. J. Li, F. J. Chen, X. Y. Zhu, J. Q. Dai, Y. F. Li, Z. Yang, X. J. Yan, J. W. Song, Y. B. Wang, E. Hitz, W. Luo, M. H. Lu, B. Yang and L. B. Hu, *Adv. Engergy Mater.*, 2018, **8**.1702884.
13. Y. Yang, R. Q. Zhao, T. F. Zhang, K. Zhao, P. S. Xiao, Y. F. Ma, P. M. Ajayan, G. Q. Shi and Y. S. Chen, *Acs Nano*, 2018, **12**, 829-835.
14. V. D. Dao and H. S. Choi, *Global Challenges*, 2018, **2**.
15. Q. M. Chen, Z. Q. Pei, Y. S. Xu, Z. Li, Y. Yang, Y. Wei and Y. Ji, *Chem. Sci.*, 2018, **9**, 623-628.
16. M. W. Zhu, Y. J. Li, G. Chen, F. Jiang, Z. Yang, X. G. Luo, Y. B. Wang, S. D. Lacey, J. Q. Dai, C. W. Wang, C. Jia, J. Y. Wan, Y. G. Yao, A. Gong, B. Yang, Z. F. Yu, S. Das and L. B. Hu, *Adv. Mater.*, 2017, **29**.
17. J. L. Yang, Y. S. Pang, W. X. Huang, S. K. Shaw, J. Schiffbauer, M. A. Pillers, X. Mu, S. R. Luo, T. Zhang, Y. J. Huang, G. X. Li, S. Ptasinska, M. Lieberman and T. F. Luo, *Acs Nano*, 2017, **11**, 5510-5518.
18. N. Xu, X. Z. Hu, W. C. Xu, X. Q. Li, L. Zhou, S. N. Zhu and J. Zhu, *Adv. Mater.*, 2017, **29**.
19. H. Ghasemi, G. Ni, A. M. Marconnet, J. Loomis, S. Yerci, N. Miljkovic and G. Chen, *Nat. Commun.*, 2014, **5, 4449**.
20. Y. Liu, S. Yu, R. Feng, A. Bernard, Y. Liu, Y. Zhang, H. Duan, W. Shang, P. Tao, C. Song and T. Deng, *Adv. Mater.*, 2015, **27**, 2768-2774.
21. G. Ni, G. Li, S. V. Boriskina, H. X. Li, W. L. Yang, T. J. Zhang and G. Chen, *Nat. Energy*, 2016, **1, 16126**.
22. Y. Wang, L. Zhang and P. Wang, *ACS Sustainable Chem. Eng.*, 2016, **4**, 1223-1230.
23. L. Zhou, Y. Tan, J. Wang, W. Xu, Y. Yuan, W. Cai, S. Zhu and J. Zhu, *Nat. Photonics*, 2016, **10**, 393.
24. L. Zhou, Y. Tan, D. Ji, B. Zhu, P. Zhang, J. Xu, Q. Gan, Z. Yu and J. Zhu, *Sci. Adv.*, 2016, **2, e1501227**.
25. Q. Jiang, L. Tian, K. K. Liu, S. Tadepalli, R. Raliya, P. Biswas, R. R. Naik and S. Singamaneni, *Adv. Mater.*, 2016, **28**, 9400-9407.
26. A. Guo, X. Ming, Y. Fu, G. Wang and X. Wang, *ACS Appl. Mater. Interfaces*, 2017, **9**, 29958-29964.
27. X. Z. Hu, W. C. Xu, L. Zhou, Y. L. Tan, Y. Wang and J. Zhu, *Adv. Mater.*, 2017, **29**, 1604031.
28. L. Zhou, S. D. Zhuang, C. Y. He, Y. L. Tan, Z. L. Wang and J. Zhu, *Nano Energy*, 2017, **32**, 195-200.
29. W. C. Xu, X. Z. Hu, S. D. Zhuang, Y. X. Wang, X. Q. Li, L. Zhou, S. N. Zhu and J. Zhu, *Adv. Energy Mater.*, 2018, **8**, 1702884.

Journal of Materials Chemistry A Accepted Manuscript

View Article Online
DOI: 10.1039/C8TA03280G

Published on 06 June 2018. Downloaded by UNIVERSITY OF SOUTH AUSTRALIA on 08/06/2018 02:58:14.

30. J. D. Yao and G. W. Yang, *J. Mater. Chem. A*, 2018, **6**, 3869-3876.
31. J. D. Yao, Z. Q. Zheng and G. W. Yang, *Nanoscale*, 2018, **10**, 2876-2886.
32. J. D. Yao, Z. Q. Zheng and G. W. Yang, *Nanoscale*, 2017, **9**, 16396-16403.
33. X. Q. Li, R. X. Lin, G. Ni, N. Xu, X. Z. Hu, B. Zhu, G. X. Lv, J. L, Li, S. N. Zhu and J. Zhu, *Natl. Sci. Rev.*, 2018, **5**, 70-77.
34. X. Q. Li, W. C. Xu, M. Y. Tang, L. Zhou, B. Zhu, S. N. Zhu and J. Zhu, *Proc. Natl. Acad. Sci. USA*, 2016, **113**, 13953-13958.
35. H. Lee, S. M. Dellatore, W. M. Miller and P. B. Messersmith, *Science*, 2007, **318**, 426-430.
36. H. Lee, J. Rho and P. B. Messersmith, *Adv. Mater.*, 2009, **21**, 431-434.
37. Y. L. Liu, K. L. Ai and L. H. Lu, *Chem. Rev.*, 2014, **114**, 5057-5115.
38. H. L. Xu, X. K. Liu and D. Y. Wang, *Chem. Mater.*, 2011, **23**, 5105-5110.
39. C. Zhang, Y. Ou, W. X. Lei, L. S. Wan, J. Ji and Z. K. Xu, *Angew. Chem. Int. Ed.*, 2016, **55**, 3054-3057.
40. L. Li, B. Yan, J. Yang, L. Chen, H. Zeng, *Adv. Mater*. **2015**, *27*, 1294.
41. Y. L. Liu, K. L. Ai, J. H. Liu, M. Deng, Y. Y. He and L. H. Lu, *Adv. Mater.*, 2013, **25**, 1353-1359.
42. Q. Tian, M. Tang, Y. Sun, R. Zou, Z. Chen, M. Zhu, S. Yang, J. Wang, J. Wang and J. Hu, *Adv. Mater.*, 2011, **23**, 3542-3547.
43. J. Xu, X. Li, X. Wu, W. Wang, R. Fan, X. Liu and H. Xu, *J. Phys. Chem. C*, 2016, **120**, 12666-12672.
44. J. D. Yao and G. W. Yang, *Small*, 2018, 14, 170452.
45. J. D. Yao, Z. Q. Zheng and G. W. Yang, *Adv. Funct. Mater*. 2017, **27**, 1701823.
46. L. L. Zhang, J. Xing, X. L. Wen, J. W. Chai, S. J. Wang and Q. H. Xiong, *Nanoscale*, 2017, 9, 12843-12849.
47. X. Z. Wang, Y. R. He, X. Liu, G. Cheng, J. Q. Zhu, *Appl. Energy*, 2017, **195**, 414-425.

Journal of Materials Chemistry A Accepted Manuscript

View Article Online
DOI: 10.1039/C8TA03280G

Table of Content

Inspired by kerosene oil lamp, a highly efficient solar-evaporation system with evaporation surface located above bulk water surface is realized.



Published on 06 June 2018. Downloaded by UNIVERSITY OF SOUTH AUSTRALIA on 08/06/2018 02:58:14.

Journal of Materials Chemistry A Accepted Manuscript